Energy & Environmental Science

COMMUNICATION

View Article Online
View Journal | View Issue

Cite this: *Energy Environ. Sci.*, 2019, **12**, 2185

Received 2nd March 2019,
Accepted 20th June 2019

DOI: 10.1039/c9ee00705a

rsc.li/ees

Biohybrid photoheterotrophic metabolism for significant enhancement of biological nitrogen fixation in pure microbial cultures†

Bo Wang, ‡[ab] Kemeng Xiao, ‡[b] Zhifeng Jiang, [cd] Jianfang Wang, *[e] Jimmy C. Yu *[a] and Po Keung Wong *[bf]

We induce the coating of biocompatible cadmium sulfide (CdS) nanoparticles (NPs) on the living cell surface of a versatile photoheterotrophic bacterium, *Rhodopseudomonas palustris*. The photo-induced electrons from the CdS NPs significantly improve the biological nitrogen fixation in pure cultures of *R. palustris*, as shown by increased nitrogenase activity, additional H_2 evolution, elevated reducing equivalents, and increased intracellular ammonia and L-amino acids. As a result, an additional 153% of solid biomass is accumulated by the biohybrid cells, with outstanding photosynthetic efficiency of 6.73% and a nearly unaffected malate usage efficiency of 0.06 g h^{-1}. The number of NPs and the cross-membrane interface both play important roles in the efficient generation and transduction of electrons. The biohybrid cells continuously fix N_2 when sufficient N is available, thus revealing excessive reducing power. The Calvin cycle also contributes 28.1% to the additional solid biomass in the presence of available CO_2. The CdS-coated photoheterotrophic cells exhibit excellent practical feasibility with an industrial waste carbon source under a solar/dark cycle. This study provides a facile and expandable strategy for other studies of visible-light-driven ambient N_2 fixation and advanced solar-to-chemical conversion.

Broader context

Nitrogen fixation, both through the industrial Haber–Bosch process and natural biological processes, has profound effects on the world's ecology and economy and the agriculture and food industries. However, the Haber–Bosch process requires harsh synthetic conditions and relies heavily upon unsustainable fossil fuels. Biological nitrogen fixation is limited by the complex catalytic mechanism and low efficiency. Emerging N_2 fixation studies in chemical and material sciences face great challenges as a result of poor chemical selectivity and productivity. Photosynthetic biohybrid systems, which combine the advantages of photocatalysts and biological systems, have become a hot topic. However, current photosynthetic biohybrid systems have only reached the proof-of-concept stage due to their dependence on enzyme purification and harsh preparation conditions for uncommon microorganisms. In this study, CdS nanoparticles are coated on the surface of a widely applied photoheterotroph, *Rhodopseudomonas palustris*. The biohybrid cells in pure culture exhibit outstanding N_2 fixation efficiency and great practical feasibility using solar light and an industrial waste carbon source. This study provides a new insight into the design of semiartificial photosynthetic systems for ambient N_2 fixation and solar-to-chemical conversion studies.

Introduction

Nitrogen fixation plays a critical role in the biogeochemical cycle and greatly affects the global ecology and economy and the agriculture and food industries.[1–3] The wide application of the industrial Haber–Bosch process has contributed greatly to the development of the human population *via* the production of nitrogen fertilizers.[4,5] However, the process requires harsh synthetic conditions and relies heavily on energy input derived mainly from unsustainable fossil fuels,[6,7] which makes it costly and environmentally hazardous.[8] Well-established biological systems can conduct N_2 fixation under ambient conditions,[9] and the biologically fixed N_2 provides about 65% of the biosphere's available nitrogen and 50% of the earth's current food demand.[4,10] However, the complex enzymatic system and catalytic mechanism hinders efforts to develop effective methods to improve the conversion efficiency.[11,12] Intensive efforts have been made in chemical and materials sciences, including N_2

[a] *Department of Chemistry, The Chinese University of Hong Kong, Shatin, New Territories, Hong Kong, 999077, China. E-mail: jimyu@cuhk.edu.hk*
[b] *School of Life Sciences, The Chinese University of Hong Kong, Shatin, New Territories, Hong Kong, 999077, China. E-mail: pkwong@cuhk.edu.hk*
[c] *Institute for Energy Research, Jiangsu University, Zhenjiang, 212013, China*
[d] *School of Energy and Environment, City University of Hong Kong, Kowloon, Hong Kong, 999077, China*
[e] *Department of Physics, The Chinese University of Hong Kong, Shatin New Territories, Hong Kong, 999077, China. E-mail: jfwang@phy.cuhk.edu.hk*
[f] *Institute of Environmental Health and Pollution Control, School of Environmental Science and Engineering, Guangdong University of Technology, Guangzhou, 510006, China*

† Electronic supplementary information (ESI) available. See DOI: 10.1039/c9ee00705a

‡ These authors contributed equally.

reduction studies on transition metal catalysts,[13,14] electrocatalysts[15] and photocatalysts.[16,17] Although they have shown efficient energy harvesting, the poor chemical selectivity of the artificial catalysts severely limits the conversion efficiency.[18,19] The extremely strong triple bond in the elemental nitrogen and the multi-step kinetic processes from N_2 to ammonia (NH_4^+) both result in an inevitable waste of energy and low productivity.[20] Therefore, huge challenges remain for both natural (biotic) and artificial (abiotic) catalytic systems.

Semiartificial photosynthetic systems that integrate inorganic materials and biological systems for solar-to-chemical (S2C) and solar-to-fuel (S2F) conversion have recently received considerable attention.[21–26] These biohybrid systems convert solar/electrical energy into chemicals with high specificity and conversion efficiency, surpassing those of the biological and chemical routes alone.[27,28] For example, light-driven N_2 reduction is achieved by a delicately fabricated semiconductor–nitrogenase complex.[3] However, the cost of enzyme purification and the low stability of the cell-free system pose great challenges to its practical applications. An electrode with hydrogen evolution activity has also been integrated with a chemoautotrophic bacterium, *Xanthobacter autotrophicus*, to realize improved N_2 fixation and solid biomass synthesis.[22] However, cultivation of the special chemoautotroph is tightly constrained by the available inorganic energy flows and the ability to maintain strict anaerobic or microaerobic conditions. Therefore, the documented prototypic biohybrid systems would encounter great difficulties in mass production and real-life application. To develop a practical biohybrid system for N_2 fixation and S2C conversion, the common N_2 fixing phototrophs are a preferable choice.[29–31]

In this study, we demonstrate the construction of cadmium sulfide (CdS) coated photoheterotrophic cells to enhance N_2 fixation *via* a series of facile strategies. We induce the coating of biocompatible CdS nanoparticles (NPs) on the living cell surface of a versatile photoheterotrophic bacterium, *Rhodopseudomonas palustris*, which has been widely applied in the food industry, in waste water treatment, in the production of valuable chemicals, and in environmental remediation.[29] With efficient stimulation of photo-induced electrons from the CdS NPs, the biohybrid cells in the pure culture exhibit significantly enhanced performance in N_2 fixation and solid biomass production. The mechanism is systematically investigated, and the feasibility of the CdS-coated photoheterotrophic cells for practical application is demonstrated.

Results and discussion

The optimal Cd^{2+} concentration for CdS-coating is studied in an N-sufficient medium (MMN, Table S1, ESI†) using cysteine (Cys) as the sulfur source.[32] 0.25 mM $Cd(NO_3)_2$ is used because 90.26% of the Cd^{2+} could be effectively precipitated (Table S2, ESI†). High-resolution transmission electronic microscopy (HRTEM) shows that well-distributed black dots formed on the bacterial surface (Fig. 1a). The thin-sectioned (70 nm) sample shows that the particles are all closely connected to the cell surface and not dispersed elsewhere (Fig. 1b). The high angle annular dark field (HAADF) STEM and energy dispersive spectrometer (EDS) mapping images (Fig. 1b inset) confirm that the NPs are only distributed on the cell surface and consist of Cd and S elements. The bacterial membrane is crossed by the NP clusters with an average size below 20 nm (Fig. 1c), which indicates the generation of a nanomaterial–cell interface. According to the JCPDS No. 80-10019,[25] the lattice fringes of the NPs (Fig. 1c, inset) are consistent with the (111) plane of CdS. Energy-dispersive X-ray spectroscopy (EDX) of the NPs further confirms that the NPs' major elements are Cd and S (Fig. 1d). The surface CdS NPs are further isolated from the cell membrane (ESI†). Consistent with previous reports,[24,33] the UV-vis spectrum (Fig. 1e) shows that isolated CdS NPs are responsive to visible light ($\lambda > 420$ nm). According to the valence band (1.62 eV *vs.* NHE) measured by X-ray photoelectron spectroscopy (XPS) and the bandgap (E_g) estimated from the UV-vis spectrum, the conduction band of the isolated CdS NPs is −0.56 eV (*vs.* NHE). The photoelectrochemical (PEC) characteristic of the isolated CdS NPs reveals good electron producing ability under visible light (VL) irradiation (Fig. 1f). Therefore, a high density of CdS NPs with good electron generating efficiency are successfully coated onto the bacterial surface.

The biological N_2 fixation of the pure bacterial culture is studied in an N-deficient medium (MMG, Table S1 and Fig. S1, ESI†) with malate as the organic carbon source and 1 mM cysteine as the sacrificial agent for the photo-induced holes (h^+).[21,24,34] Under VL irradiation (80 W m^{-2} fluorescent tubes), the nitrogenase activity of CdS-coated *R. palustris* is consistently higher than that of the natural cells (Fig. 2a) and nearly double (~600 nmol C_2H_4 produced h^{-1} mg^{-1} cell) at 18 h. The enhanced H_2 evolution in the biohybrid cells (Fig. 2b) is also evidence of increased nitrogenase activity because H_2 is a byproduct of N_2 fixation.[35] A higher level of NADPH is observed during N_2 fixation in the biohybrid cells (Fig. 2c), thus revealing that excessive electrons are obtained by ferredoxin–$NADP^+$ oxidoreductase (FNR).[36,37] This result is supported by the −0.56 eV conduction band of the CdS NPs, which meets the reduction potential requirement to push the photosystem for final $NADP^+$ reduction (−0.32 eV). The improved performance of the nitrogenase and FNR illustrates that more reducing powers are received by their common electron supplier, ferredoxin (Fd), from the photosynthetic electron transport (PET) chain.[37]

The dramatic initial decrease in NH_4^+ in the natural cells (Fig. 2d) indicates that the NH_4^+ is rapidly consumed during the adaptation to the N-deficient environment. The later recovery reveals the replenishment of NH_4^+ by the fixed N_2. In contrast, NH_4^+ initially accumulates rapidly in the biohybrid cells (Fig. 2d). The decrease that followed reveals the simultaneous bioconversion of products that contain NH_4^+. Intracellular L-amino acids are promoted in the biohybrid cells (Fig. 2e), thus indicating that more NH_4^+-containing products, such as protein, lipid and bacteriochlorophyll,[38] are converted from fixed N_2 for the biosynthesis. Elemental analyzer-isotopic ratio mass spectrometry (EA-IRMS) using 15-N_2 as the purge gas (purity >99.9%) (ESI†) shows the signal of $\delta^{15}N$ (mass-to-charge ratio = 29) for both

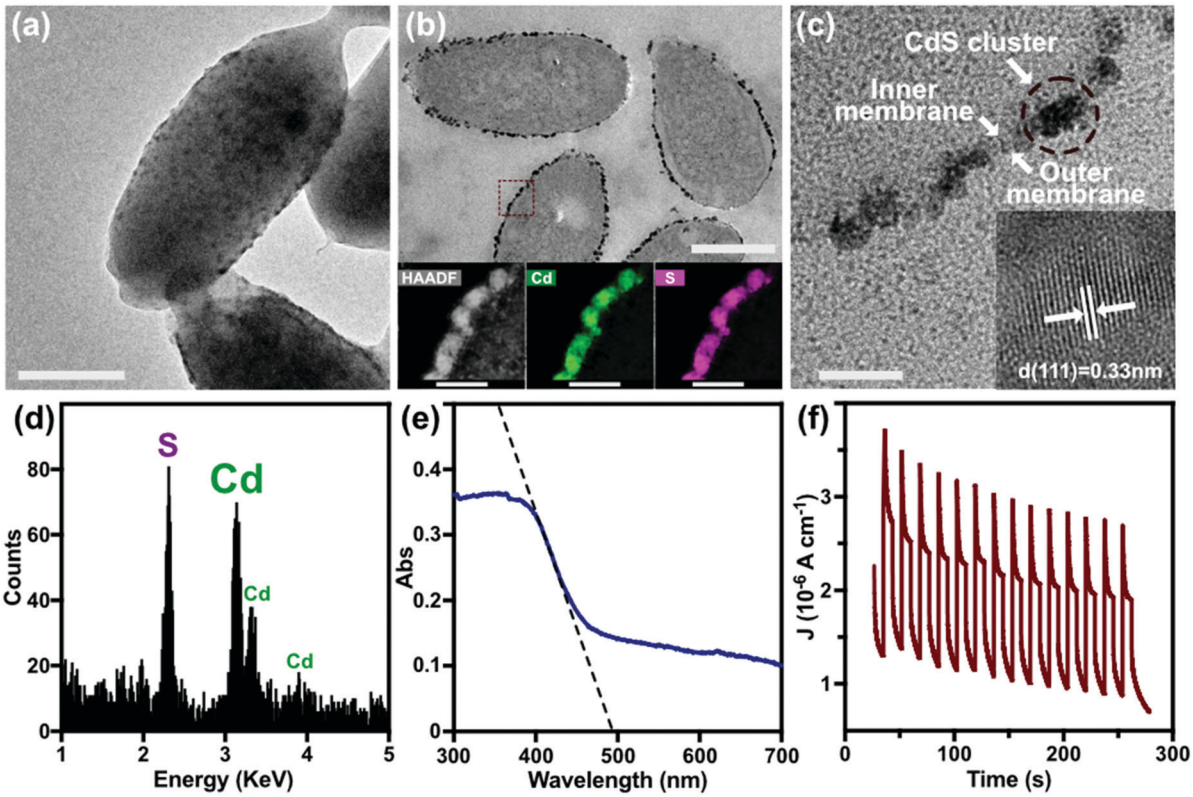

Fig. 1 (a) High-resolution transmission electronic microscopy of (a) non-sectioned and (b) thin-sectioned CdS-coated cells and (c) NP clusters across the cell membrane. (d) Energy-dispersive X-ray spectroscopic pattern showing the major elements of the NPs. (e) UV-vis spectrum of an isolated CdS NP. (f) Transition photocurrent of isolated CdS NPs under visible light irradiation. Scale bars: (a and b) 500 nm; figure inset in (b) 50 nm; (c) 50 nm.

the natural and biohybrid cells (Fig. 2f and g). A higher ratio of $^{15}N/^{14}N$ is exhibited in the biohybrid cells. Therefore, gaseous N_2 is confirmed to be fixed for biosynthesis, and the biohybrid cells possess greater N_2 fixation ability. Under VL irradiation and a N_2 environment, the solid biomass accumulated by the biohybrid cells (3.44 g L^{-1}) is 253% that of the natural cells (1.35 g L^{-1}, Fig. 2h). This productivity surpasses the performance seen when supplied with 10 mM ammonia, whereas the mass of the natural cells is only higher than when supplied with 2.5 mM ammonia (Fig. S2, ESI†). The huge gap between the Ar and N_2 groups under VL suggests that the fixed N_2 makes a major contribution to the solid biomass. It also proves the limited nutritional function (as a source of N) of glutamic acid, which plays an essential role in the conversion of NH_4^+ into amino acids and in the regulation of nitrogenase activity.[38,39] In darkness, no difference in productivity is observed between the natural and biohybrid cells (Fig. 2h) or in the neglectable H_2 evolution and intracellular ammonia variation (Fig. S3, ESI†). The results indicate that no additional energy for biosynthesis is obtained by the CdS-coated cells. The small difference between the Ar and N_2 groups in darkness also demonstrates the important role played by light, which not only induces the electrons from the surface-coated CdS NPs, but also provides the adenosine triphosphate (ATP) for the nitrogenase to fix N_2.[39]

According to the calculation of photosynthetic efficiency (PE) (Tables S3–S5, ESI†), the CdS-coated *R. palustris* shows a PE of 6.73%, which is 186% higher than that of the natural cells (2.35%) and superior to that of many photoheterotrophic bacteria.[40] In addition, the nearly unaffected malate consumption efficiency (Table S4, ESI†) reveals that the simultaneous heterotrophic metabolism works stably with the photoactivated CdS NPs, which contribute mostly to the increase in biomass production by improving the PE. With help from the surface-coated CdS NPs, the energy from light and light-induced electrons contributed 80.5% to the solid biomass production. Thus, it is reasonable to infer that the photo-induced electrons from the surface-coated CdS NPs endow the biohybrid cells with greater N_2 fixation capacity, bringing the bacteria more substrates for biosynthesis and resulting in a significant enhancement in S2C conversion efficiency and PE.

Under VL irradiation, a positive relationship is found between productivity and the number of coated CdS NPs (Fig. 3a), thus illustrating that a greater number of surface NPs provides more exogenous bioavailable energy to *R. palustris*. In darkness, no difference in productivity is observed between the groups, thus demonstrating that the surface-coated CdS NPs could not provide energy without light irradiation. The potential cytotoxicity of the CdS NPs is studied in nutrient broth (Lab M, Lancashire, UK) in darkness to eliminate the growth promoting function of the CdS NPs and provide sufficient nutrients for bacterial growth. No cytotoxicity is found from the similar growth curves of the biohybrid cells with different amounts of CdS NPs

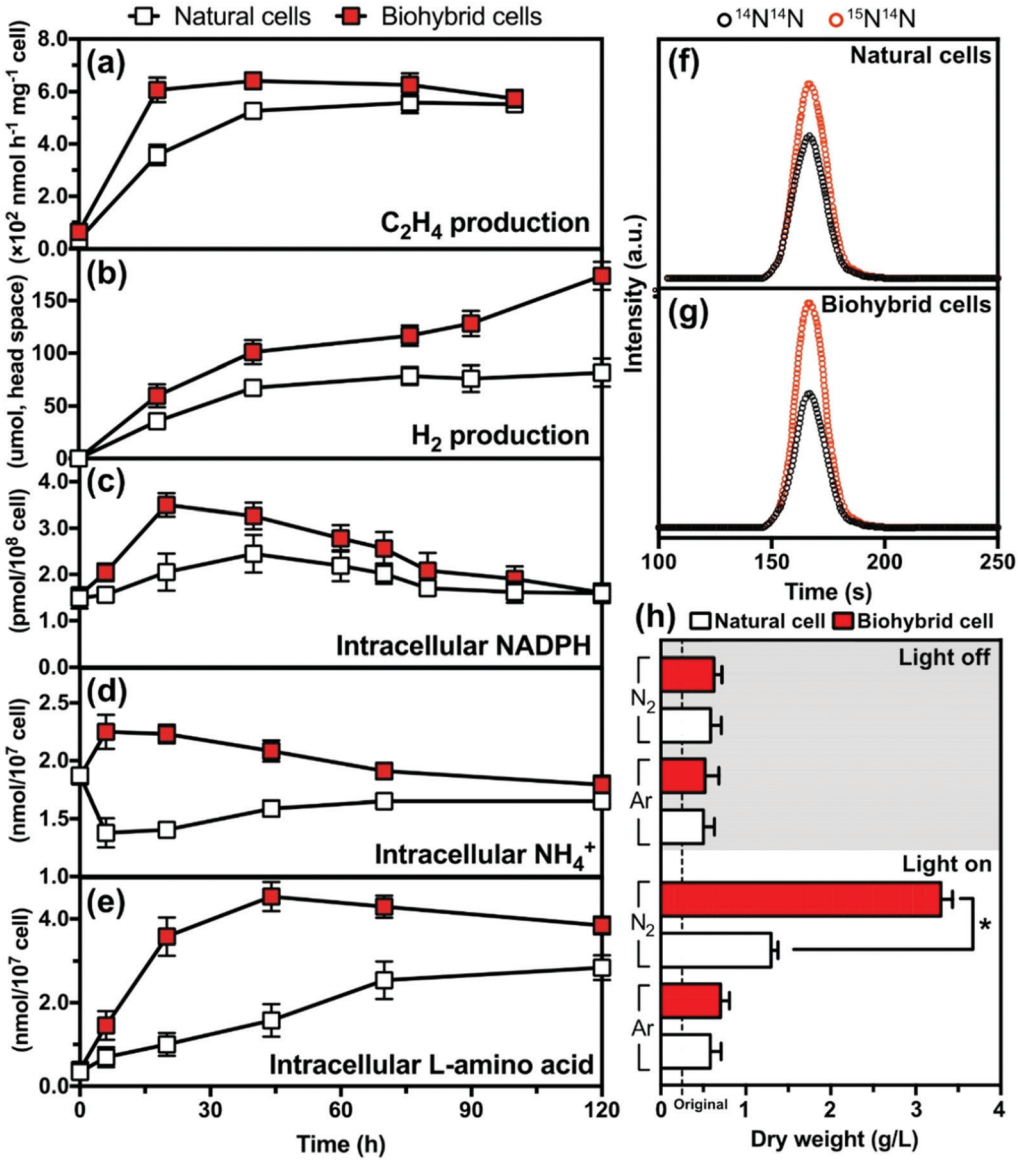

Fig. 2 N_2 fixation of natural and biohybrid cells in an N-deficient medium with malate as the carbon source (MMG medium, Table S1, ESI†). (a) Nitrogenase activity measured by acetylene/ethylene assay in the headspace, (b) H_2 evolution in the vial's headspace, (c) intracellular NADPH level, (d) intracellular NH_4^+ concentration, and (e) intracellular L-amino acid concentration. Elemental analyzer-isotopic ratio mass spectrometry of the $^{15}N^{14}N$ and $^{14}N^{14}N$ from the (f) natural cells and (g) biohybrid cells in the $^{15}N_2$ isotope study, and (h) dry weight of the solid biomass after 120 h N_2 fixation under Ar/N_2. Dashed line: starting value. An asterisk mark indicates statistical significance ($p < 0.05$).

(Fig. S4, ESI†). The greatest concentration of loaded CdS NPs (0.25 mM) also leads to the strongest stimulation of the cellular reducing equivalent (NADPH) (Fig. 3b), which suggests that more electrons could be acquired for biosynthesis by the PET chain. It is therefore further confirmed that the photo-induced electrons from the coated CdS NPs are integrated with the photosynthetic N_2 fixation pathway. A slight improvement in solid biomass production is observed in CdS-coated *R. palustris* as the cysteine concentration increased (Fig. 3c). However, no great difference is seen in the corresponding groups of natural cells. This result not only proves the efficient charge separating function of cysteine as the hole sacrificial agent,[21] but also demonstrates the limited contribution of the NH_4^+-containing cysteine as a source of N.

The solid biomass obtained from the natural cells simply mixed with 0.25 mM isolated or chemically synthesized CdS (ESI†) is much lower than the cells with CdS NPs coated on the membrane (Fig. 3d). This finding indicates that the cross-membrane CdS–cell interface plays an important role in the efficient transduction of photo-induced electrons in the biological pathway. In addition, the apparent inhibiting effect of the electron scavenger on the productivity of the biohybrid cells (Fig. 3d) further confirms the transduced electrons as the source of exogeneous energy for biomass synthesis.

N_2 fixation is further investigated in an N-sufficient medium (MMN, Table S1, ESI†). No difference is observed in the natural cells cultured under Ar and N_2 for either cellular NH_4^+

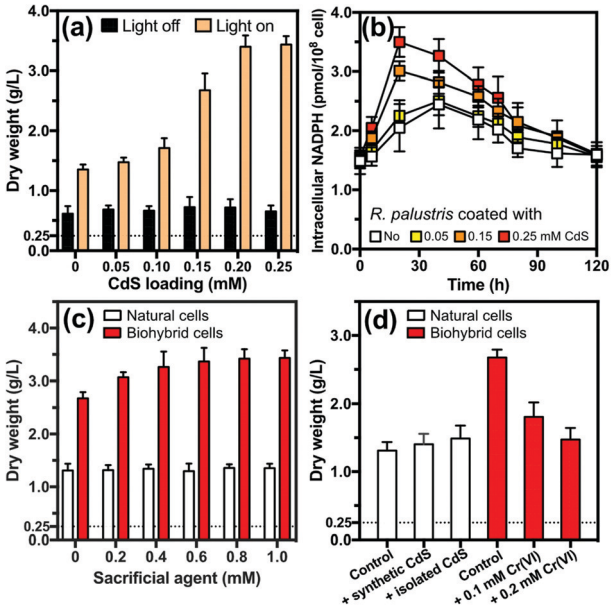

Fig. 3 (a) Productivity and (b) intracellular NADPH concentration of *R. palustris* coated with various amounts of CdS, (c) obtained solid biomass of natural and biohybrid cells supplemented with different concentrations of cysteine, and (d) productivity of *R. palustris* separated with CdS and biohybrid cells added with electron scavenger. Dashed line: starting value.

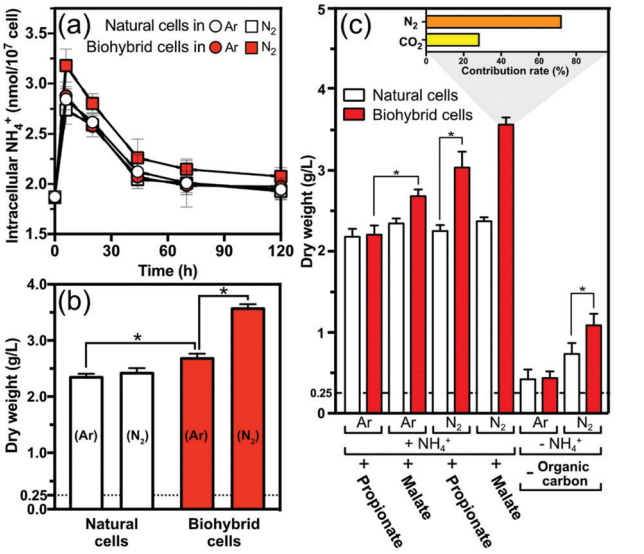

Fig. 4 (a) Variation in intracellular NH_4^+ concentration and (b) solid biomass production by CdS-coated *R. palustris* and natural cells in N-sufficient medium under N_2 and Ar atmospheres, and (c) solid biomass production by natural and biohybrid cells in an N-sufficient medium with propionate or malate and N-deficient medium without any organic carbon sources (photoautotrophic medium) under Ar and N_2 atmospheres, reaction time: 120 h. Dashed line: starting value. An asterisk indicates statistical significance ($p < 0.05$).

alteration or the produced biomass (Fig. 4a and b). This result is reasonable because the nitrogenase is relatively inactive in the presence of sufficient available ammonium.[41,42] However, the *R. palustris* coated with CdS NPs still generates more NH_4^+ and solid biomass under N_2 and light (Fig. 4a and b), and more H_2 is produced than in the parallel group under Ar (Fig. S5, ESI†), revealing that nitrogenase still works. Because the photo-induced electrons could bring additional reducing power and potential harmful effects to the cell when breaking the redox balance,[43] it is reasonable to infer that the biohybrid cells are driven to release the excessive reducing power in the form of NH_4^+ generation.

Under Ar, we are interested to observe 14.3% greater productivity in the biohybrid cells than in the natural cells (Fig. 4b). This result indicates that certain sources other than N_2 contribute to the additional biosynthesis. The oxidation of malate releases a considerable amount of CO_2,[31] it is therefore suspected that the CO_2-reducing Calvin cycle[44] plays a role in the promoted biosynthesis. When malate is substituted by equimolar non-CO_2 releasing propionate[31] (in an MPN medium, Table S1, ESI†) under Ar, no difference in biomass is found between the CdS-coated *R. palustris* and the natural cells (Fig. 4c), which indicates that no factors other than the available N_2 and CO_2 can affect the biosynthesis. When the propionate is switched to malate, an additional 21.6% of biomass is accumulated in the CdS-coated *R. palustris*, confirming the contribution of CO_2 fixation to biosynthesis. The biomass productivity of the natural and biohybrid cells using propionate without providing NH_4^+ (in MPG medium, Table S1, ESI†) is also studied. As with malate, the produced biomass is much higher in the biohybrid cells under N_2 (Fig. S6, ESI†). The lower biomass productivity of the biohybrid cells under N_2 with propionate again indicates the participation of the Calvin cycle in the biosynthesis when CO_2 is available. As an NADPH-consuming process,[44] the active Calvin cycle further proves the existence of the excessive reducing power converted from the surface-coated CdS NPs. In the presence of propionate under N_2, an additional 34.9% biomass is obtained in the biohybrid cells (Fig. 4c), which suggests that the additional biomass is contributed by N_2 fixation alone. As a result of the simultaneous work of nitrogenase and the Calvin cycle, an additional 1.20 g L^{-1} of biomass (Fig. 4c) is achieved when using malate under a N_2 atmosphere. By calculating the individual contribution, the proportions of fixed N_2 and CO_2 are roughly evaluated to be 71.9% and 28.1%, respectively (Fig. 4c, inset).

Without providing organic carbon and nitrogen sources (photoautotrophic medium, Table S1, ESI†), much lower productivity is observed in both natural and biohybrid cells (Fig. 4c). This phenomenon is normal because the *R. palustris* cannot rely upon the CO_2 as the sole carbon source for effective photoautotrophic growth.[45] However, when N_2 is available, a significant improvement in productivity is still observed in the biohybrid cells (Fig. 4c), with additional H_2 evolution and a higher intracellular concentration of ammonia (Fig. S7, ESI†). These results demonstrate that the surface-coated CdS NPs endow *R. palustris* with greater photoautotrophic growth ability by promoting bacterial N_2 fixation activity.

Based on these results, a mechanism is proposed for the enhanced N_2 fixation and biomass conversion in CdS-coated

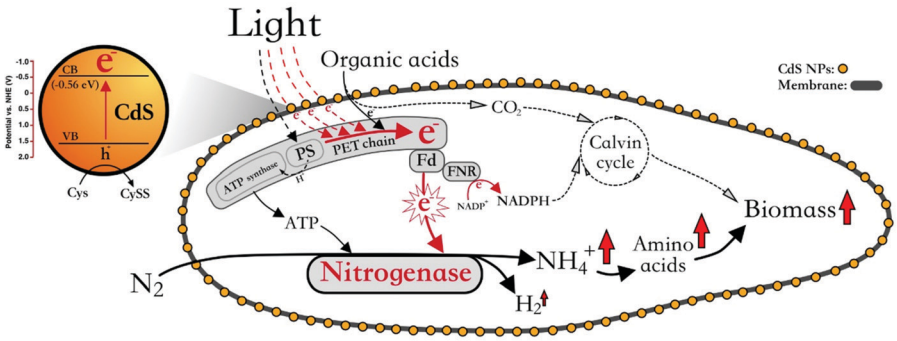

Fig. 5 Schematic illustration of enhanced N_2 fixation and S2C conversion in the CdS-coated *R. palustris* cell (PS: photosystem. PET chain: photosynthetic electron transfer chain. Fd: ferredoxin. FNR: ferredoxin–$NADP^+$ oxidoreductase. Cys: cysteine. CySS: cystine.).

R. palustris (Fig. 5). Under VL irradiation, the surface-coated CdS NPs efficiently generate electrons with sufficient energy. Efficient charge separation and electron transduction are achieved by the cysteine and the cross-membrane interface between the nanomaterial and the cell. The photo-induced electrons integrate with the PET chains and finally reach the nitrogenase and $NADP^+$ through the ferredoxin and FDR, thus generating excessive intracellular reducing power. By promoting the fixation of atmospheric N_2, the nitrogenase releases the reducing power and simultaneously generates more substrates for biosynthesis, thus enhancing the photosynthetic efficiency. In the presence of available CO_2, the Calvin cycle also contributes to biomass production. The enhanced N_2 fixation works well with the heterotrophic metabolism and finally achieves a significant enhancement in biomass production.

The feasibility of applying CdS-coated photoheterotrophic cells in pure culture for practical application is investigated (ESI†).

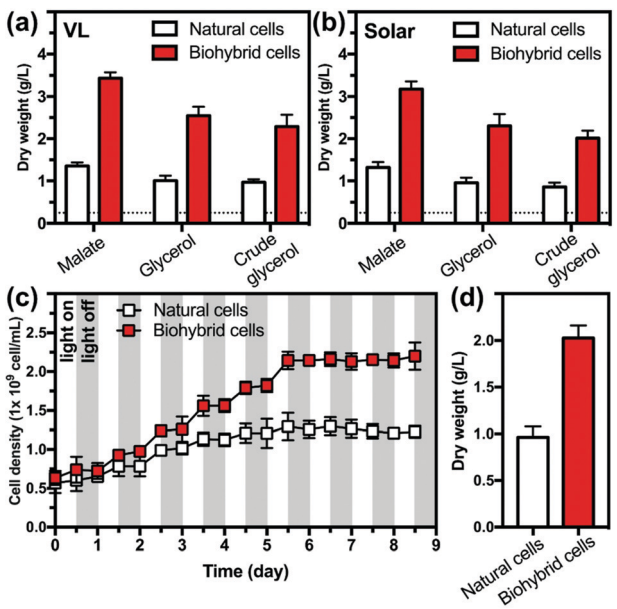

Fig. 6 Solid biomass production of the natural and biohybrid cells using malate, glycerol, and crude glycerol under (a) VL and (b) solar light. Dashed line: starting value. (c) Variation in cell density and (d) final yield of solid biomass of natural and biohybrid cells using crude glycerol under solar irradiation.

Although the productivity from (crude) glycerol (with an equal molar of carbon as the malate) is lower than that from malate under VL and solar irradiation (Fig. 6a and b), *R. palustris* coated with CdS NPs still exhibits improved solid biomass productivity. Using a crude glycerol under 12h:12h light/dark cycle (ESI†), the cell density of the biohybrid cells is consistently higher than the natural cells (Fig. 6c). Finally, the biomass obtained by the biohybrid cells is nearly doubled (Fig. 6d). In addition, about 85% of the respiration activity remains in the biohybrid cells after 9 days (Fig. S8a, ESI†), and HRTEM confirms that the coated CdS NPs are still connected to the bacterial membrane (Fig. S8b, ESI†). The overall healthy green staining also proves the good membrane integrity of the cells (Fig. S8c, ESI†). It can also be observed that the concentration of Cd^{2+} released from the CdS NPs is below the detection limit of atomic absorption spectroscopy (AAS, Hitachi Z2300, Japan), which indicates that the system is not harmful to the environment. Therefore, the stable CdS-coated photoheterotrophic bacterium possesses great feasibility for practical applications using free solar energy and cheap industrial waste carbon sources.

Conclusions

A CdS-photoheterotrophic biohybrid system is constructed *via* facile strategies for enhancement of N_2 fixation and S2C conversion. The photo-induced electrons from the surface-coated CdS NPs efficiently promote bacterial N_2 fixation both with and without ammonium, thus leading to improved biomass synthesis. Driven by the exogeneous reducing power, the CdS-coated *R. palustris* in pure cultures shows greater photoautotrophic survivability and excellent feasibility for practical application using solar light and an industrial waste carbon source. The strategy reported here can also be expanded to construct other photoheterotroph-based biohybrid systems for N_2 fixation and advanced S2C studies.

Conflicts of interest

The authors declare no conflict of interest.

Acknowledgements

Bo Wang appreciates the assistance from Prof. Xuelu Wang from Huazhong Agricultural University and Prof. Zhonghua Cai from Tsinghua University, for the nitrogenase activity assay and the 15-N_2 isotope labelling experiment. This study was supported by a grant from the Research Grants Council of the Hong Kong Special Administrative Region (Project No. 14308018) to Jimmy C. Yu. This project was also supported by a grant from Science Faculty, The Chinese University of Hong Kong (CUHK) for Research on Environmental and Sustainability to J. F. Wang, J. C. Yu and P. K. Wong, and a Technology Business Development Fund (TBF18SCI006) of CUHK to P. K. Wong. Dr Zhifeng Jiang gratefully acknowledges financial support from the National Natural Science Foundation of China (21706102) and the Natural Science Foundation of Jiangsu Province (BK20170527).

References

1 N. Gruber and J. N. Galloway, *Nature*, 2008, **451**, 293–296.
2 J. N. Galloway, A. R. Townsend, J. W. Erisman, M. Bekunda, Z. C. Cai, J. R. Freney, L. A. Martinelli, S. P. Seitzinger and M. A. Sutton, *Science*, 2008, **320**, 889–892.
3 K. A. Brown, D. F. Harris, M. B. Wilker, A. Rasmussen, N. Khadka, H. Hamby, S. Keable, G. Dukovic, J. W. Peters, L. C. Seefeldt and P. W. King, *Science*, 2016, **352**, 448–450.
4 J. W. Erisman, M. A. Sutton, J. Galloway, Z. Klimont and W. Winiwarter, *Nat. Geosci.*, 2008, **1**, 636–639.
5 R. D. Milton, R. Cai, S. Abdellaoui, D. Leech, A. L. De Lacey, M. Pita and S. D. Minteer, *Angew. Chem., Int. Ed.*, 2017, **56**, 2680–2683.
6 A. R. Townsend and R. W. Howarth, *Sci. Am.*, 2010, **302**, 64–71.
7 D. Kim, K. K. Sakimoto, D. C. Hong and P. D. Yang, *Angew. Chem., Int. Ed.*, 2015, **54**, 3259–3266.
8 J. Kaiser, *Science*, 2001, **294**, 1268–1269.
9 R. Dixon and D. Kahn, *Nat. Rev. Microbiol.*, 2004, **2**, 621–631.
10 E. M. Lodwig, A. H. F. Hosie, A. Bordes, K. Findlay, D. Allaway, R. Karunakaran, J. A. Downie and P. S. Poole, *Nature*, 2003, **422**, 722–726.
11 D. F. Herridge, M. B. Peoples and R. M. Boddey, *Plant Soil*, 2008, **311**, 1–18.
12 D. C. Rees, F. A. Tezcan, C. A. Haynes, M. Y. Walton, S. Andrade, O. Einsle and J. B. Howard, *Philos. Trans. R. Soc., A*, 2005, **363**, 971–984.
13 K. Arashiba, Y. Miyake and Y. Nishibayashi, *Nat. Chem.*, 2011, **3**, 120–125.
14 J. S. Anderson, J. Rittle and J. C. Peters, *Nature*, 2013, **501**, 84–87.
15 R. Lan, J. T. S. Irvine and S. W. Tao, *Sci. Rep.*, 2013, **3**, 1145.
16 J. Liu, M. S. Kelley, W. Q. Wu, A. Banerjee, A. P. Douvalis, J. S. Wu, Y. B. Zhang, G. C. Schatz and M. G. Kanatzidis, *Proc. Natl. Acad. Sci. U. S. A.*, 2016, **113**, 5530–5535.
17 M. Ali, F. L. Zhou, K. Chen, C. Kotzur, C. L. Xiao, L. Bourgeois, X. Y. Zhang and D. R. MacFarlane, *Nat. Commun.*, 2016, **7**, 11335.
18 B. N. Trawick, A. T. Daniher and J. K. Bashkin, *Chem. Rev.*, 1998, **98**, 939–960.
19 A. P. Wight and M. E. Davis, *Chem. Rev.*, 2002, **102**, 3589–3613.
20 S. J. Li, D. Bao, M. M. Shi, B. R. Wulan, J. M. Yan and Q. Jiang, *Adv. Mater.*, 2017, **29**, 1700001.
21 K. K. Sakimoto, A. B. Wong and P. D. Yang, *Science*, 2016, **351**, 74–77.
22 C. Liu, K. K. Sakimoto, B. C. Colon, P. A. Silver and D. G. Nocera, *Proc. Natl. Acad. Sci. U. S. A.*, 2017, **114**, 6450–6455.
23 C. Liu, J. J. Gallagher, K. K. Sakimoto, E. M. Nichols, C. J. Chang, M. C. Y. Chang and P. D. Yang, *Nano Lett.*, 2015, **15**, 3634–3639.
24 B. Wang, C. P. Zeng, K. H. Chu, D. Wu, H. Y. Yip, L. Q. Ye and P. K. Wong, *Adv. Energy Mater.*, 2017, **7**, 1700611.
25 Z. F. Jiang, B. Wang, J. C. Yu, J. F. Wang, T. C. An, H. J. Zhao, H. M. Li, S. Q. Yuan and P. K. Wong, *Nano Energy*, 2018, **46**, 234–240.
26 Y. Honda, M. Watanabe, H. Hagiwara, S. Ida and T. Ishihara, *Appl. Catal., B*, 2017, **210**, 400–406.
27 S. N. Nangle, K. K. Sakimoto, P. A. Silveri and D. G. Nocera, *Curr. Opin. Chem. Biol.*, 2017, **41**, 107–113.
28 K. K. Saldrnoto, N. Kornienko and P. D. Yang, *Acc. Chem. Res.*, 2017, **50**, 476–481.
29 F. W. Larimer, P. Chain, L. Hauser, J. Lamerdin, S. Malfatti, L. Do, M. L. Land, D. A. Pelletier, J. T. Beatty, A. S. Lang, F. R. Tabita, J. L. Gibson, T. E. Hanson, C. Bobst, J. L. T. Y. Torres, C. Peres, F. H. Harrison, J. Gibson and C. S. Harwood, *Nat. Biotechnol.*, 2004, **22**, 55–61.
30 H. Halm, P. Lam, T. G. Ferdelman, G. Lavik, T. Dittmar, J. LaRoche, S. D'Hondt and M. M. M. Kuypers, *ISME J.*, 2012, **6**, 1238–1249.
31 O. Hadicke, H. Grammel and S. Klamt, *BMC Syst. Biol.*, 2011, **5**, 150–168.
32 H. J. Bai, Z. M. Zhang, Y. Guo and G. E. Yang, *Colloids Surf., B*, 2009, **70**, 142–146.
33 K. E. Marusak, Y. Feng, C. F. Eben, S. T. Payne, Y. Cao, L. You and S. Zauscher, *RSC Adv.*, 2016, **6**, 76158–76166.
34 Q. Z. Wang, J. H. Lian, J. J. Li, R. F. Wang, H. H. Huang, B. T. Su and Z. Q. Lei, *Sci. Rep.*, 2015, **5**, 1–9.
35 J. M. Dubbs and F. R. Tabita, *FEMS Microbiol. Rev.*, 2004, **28**, 353–376.
36 T. Y. Aw, *Physiology*, 2003, **18**, 201–204.
37 H. Haaker and J. Klugkist, *FEMS Microbiol. Lett.*, 1987, **46**, 57–71.
38 V. I. Beaumont, L. L. Jahnke and D. J. Des Marais, *Org. Geochem.*, 2000, **31**, 1075–1085.
39 P. F. Teixeira, H. Wang and S. Nordlund, *J. Bacteriol.*, 2010, **192**, 1463–1466.
40 I. Akkerman, M. Janssen, J. Rocha and R. H. Wijffels, *Int. J. Hydrogen Energy*, 2002, **27**, 1195–1208.
41 B. Masepohl, T. Drepper, A. Paschen, S. Gross, A. Pawlowski, K. Raabe, K. U. Riedel and W. Klipp, *J. Mol. Microbiol. Biotechnol.*, 2002, **4**, 243–248.
42 J. Oelze and G. Klein, *Arch. Microbiol.*, 1996, **165**, 219–225.
43 H. Zhang, P. Limphong, J. Pieper, Q. Liu, C. K. Rodesch, E. Christians and I. J. Benjamin, *FASEB J.*, 2012, **26**, 1442–1451.
44 A. Bar-Even, E. Noor, N. E. Lewis and R. Milo, *Proc. Natl. Acad. Sci. U. S. A.*, 2010, **107**, 8889–8894.
45 A. Bose, E. Gardel, C. Vidoudez, E. Parra and P. Girguis, *Nat. Commun.*, 2014, **5**, 3391–3398.